Advances in Water Resources 34 (2011) 640–648

Contents lists available at ScienceDirect

Advances in Water Resources

journal homepage: www.elsevier.com/locate/advwatres

A general analytical solution for flow to a single horizontal well by Fourier and Laplace transforms

Ching-Sheng Huang, Yu-Lin Chen, Hund-Der Yeh *

Institute of Environmental Engineering, National Chiao Tung University, 1001 University Road, Hsinchu 30039, Taiwan

ARTICLE INFO

Article history:
Received 26 August 2010
Received in revised form 23 February 2011
Accepted 23 February 2011
Available online 1 March 2011

Keywords:
Free surface equation
Unconfined aquifer
Stream depletion rate

ABSTRACT

The objective of this paper is to present an analytical solution for describing the head distribution in an unconfined aquifer with a single pumping horizontal well parallel to a fully penetrating stream. The Laplace-domain solution is developed by applying Fourier sine, Fourier and Laplace transforms to the governing equation as well as the associated initial and boundary conditions. The time-domain solution is obtained after taking the inverse Laplace transform along with the Bromwich integral method and inverse Fourier and Fourier sine transforms. The upper boundary condition of the aquifer is represented by the free surface equation in which the second-order slope terms are neglected. Based on the solution and Darcy's law, the equation representing the stream depletion rate is then derived. The solution can simulate head distributions in an aquifer infinitely extending in horizontal direction if the well is located far away from the stream. In addition, the solution can also simulate head distributions in confined aquifers if specific yield is set zero. It is shown that the solution can be applied practically to evaluate flow to a horizontal well.

1. Introduction

The stream depletion rate (SDR) is herein defined as the ratio of infiltrative water from the stream (or lake, stream, etc.) to the total amount of water produced from the pumping well. The stream depletion rate increases gradually with pumping time and finally approaches one, which reflects most of water comes from the stream, after a certain period of pumping time. Many analytical models treat the stream as a constant-head boundary to estimate stream depletion rate [e.g., 1–3,6,17,21]. Some researchers proposed to treat the stream as a variable stream stage represented by a periodic function for seasonal variations or a function changed in space and time for flood wave [7]. The articles mentioned above investigated the behavior of stream depletion rate induced from a vertical well. In addition, their mathematical model neglects vertical flow to unconfined aquifers.

Recently, the horizontal well becomes popular due to the advanced technique in drilling the wellbore. There are some advantages to use the horizontal well. For example, the cost from operating horizontal wells is half of that from vertical wells [8]. Horizontal wells have better contact with aquifers and are appropriate to install in thin aquifers. A shallow drawdown cone will be produced if adopting a long and deep horizontal well. Some semi-analytical or numerical solutions are developed to investigate the behaviors of the groundwater flow induced from horizontal wells [e.g., 9–12,20]. Zhan et al. [18] provided a method to solve the boundary problem of groundwater flow to the horizontal well. Their method is first to consider a pumping point source and then to integrate the point source solution along the well axis. Based on this approach, they developed an analytical solution for describing the groundwater flow induced from horizontal wells in a confined aquifer. Zhan and Zlotnik [19] developed a semi-analytical solution requiring numerical inversion to investigate the drawdown due to slanted wells in an unconfined aquifer. They indicated that the type curve of drawdown had three stages, including rapid increase at early time, middle flat stage and rapid increase again at late time. Sun and Zhan [13] presented semi-analytical solutions to describe the groundwater flow induced from horizontal wells in an aquitard-aquifer system beneath a water reservoir. The flow in aquitard overlying the confined aquifer is represented by a transient equation with a term accounting for the specific storage. These articles involved in horizontal wells consider the aquifer extending infinitely in horizontal direction. Thus they did not investigate the behavior of stream depletion rate induced from a horizontal well.

Tsou et al. [14] presented an analytical solution developed by Fourier transforms to describe the stream depletion rate induced from the slanted well in confined aquifers. They found that the horizontal well parallel to the stream had less time to reach quasi-steady stream depletion rate in comparison with various directions of well axis. Therefore, it is better to install the horizontal well

* Corresponding author. Fax: +886 35 726050.
E-mail address: hdyeh@mail.nctu.edu.tw (H.-D. Yeh).

0309-1708/$ - see front matter © 2011 Elsevier Ltd. All rights reserved.
doi:10.1016/j.advwatres.2011.02.015

parallel to the stream. The difference between this paper and theirs is mainly that they considered confined aquifers while this paper considers unconfined aquifers. Accordingly, their solution can not examine the effects of behaviors of unconfined aquifers on the stream depletion rate such as specific yield and well depths.

This paper develops a mathematical model for describing head distributions in unconfined aquifers for pumping from a single horizontal well parallel to the stream. A first-order free surface equation is used as the upper boundary condition. The time-domain solution of the model is derived based on the methods of Fourier sine, Fourier and Laplace transforms. This solution can be used to simulate head distribution in a confined aquifer when the specific yield is set zero or in an aquifer extending infinitely in horizontal direction if the well is located far away from the stream. Based on Darcy's law, this solution can also be used to derive an equation for estimating stream depletion rate at any time for the well installed at any location and with any length. The effects of specific yield, well depth and anisotropic hydraulic conductivity on the stream depletion rate are examined. Spatial head distributions for various depths are also investigated. In addition, the hydraulic head evaluated from the solution is compared with the observed field data of Mohamed and Rushton [12]. The solution is useful for designing a horizontal well near a stream.

2. Method

2.1. Mathematical model

Fig. 1 shows the three-dimensional (3D) conceptual model for an anisotropic unconfined aquifer with a horizontal well parallel to a fully penetrating stream. The origin of coordinate system is located at the interface between the stream and aquifer and the x axis passes through the middle of the well. The top of the stream is considered as reference datum. The thickness of the aquifer is H and the depth of the well is D as shown in Fig. 1(b). In addition, the distance measured from the stream to the well is d and the well length is L as indicated in Fig. 1(a).

Three assumptions introduced for the model are: (1) The aquifer is homogeneous. (2) The stream stage does not change during the pumping period, implying that the stream has a large quantify of water in comparison with that drawn from the well. (3) The stream bed has the same hydraulic conductivity as aquifers. Note that Intaraprasong and Zhan [7] had addressed the effects of variable stream stage and low-permeable stream bed on the stream depletion rate.

To acquire the solution for pumping from a horizontal well, we start with the development of a point source solution of the model [e.g., 14,19]. The governing equation for describing 3D transient hydraulic head distribution $h(x,y,z,t)$ in the unconfined aquifer with a point source can be expressed as

$$K_x\frac{\partial^2 h}{\partial x^2}+K_y\frac{\partial^2 h}{\partial y^2}+K_z\frac{\partial^2 h}{\partial z^2}=S_s\frac{\partial h}{\partial t}+Q\delta(x-x_0)\delta(y-y_0)\delta(z+z_0) \tag{1}$$

where K_x, K_y and K_z are hydraulic conductivities in the x, y and z direction, respectively; S_s is specific storage; Q is a positive constant pumping rate of the point source; $\delta()$ represents the Dirac delta function and (x_0,y_0,z_0) is the location of the point source.

The water table before the pumping is considered to be horizontal and thus the initial condition is formulated as

$$h=0 \quad \text{at } t=0. \tag{2}$$

The stream is hydraulic contact with the aquifer and considered as a constant-head boundary. The boundary condition at $x=0$ is therefore expressed as

$$h=0 \quad \text{at } x=0. \tag{3}$$

The remote boundary conditions in x and y directions are considered as constant-head boundaries

$$\lim_{x\to\infty} h=0, \tag{4}$$

$$\lim_{y\to\pm\infty} h=0, \tag{5}$$

where the groundwater is not affected by the pumping. Consider the aquifer lies on an impermeable layer such that

$$\frac{\partial h}{\partial z}=0 \quad \text{at } z=-H. \tag{6}$$

The equation describing the change in water table with the absence of a surface recharge can be written by neglecting the second-order terms as [16]

$$S_y\frac{\partial h}{\partial t}=-K_z\frac{\partial h}{\partial z} \quad \text{at } z=h, \tag{7}$$

where S_y is specific yield. Note that the stream provides water to the well and consequently avoids significant deformation of the free surface due to pumping. The largest drawdown due to pumping is much smaller than the aquifer thickness. The domain in z direction ($-H\sim h$) is hence approximated from $-H$ to 0, where the head distribution at $z=0$ is the water table. Eq. (7) is further simplified as [19]

$$S_y\frac{\partial h}{\partial t}=-K_z\frac{\partial h}{\partial z} \quad \text{at } z=0. \tag{8}$$

Except Eq. (3), the mathematical formulation herein is identical to Zhan and Zlotnik [19] where they considered an unconfined aquifer infinitely extending in the horizontal direction.

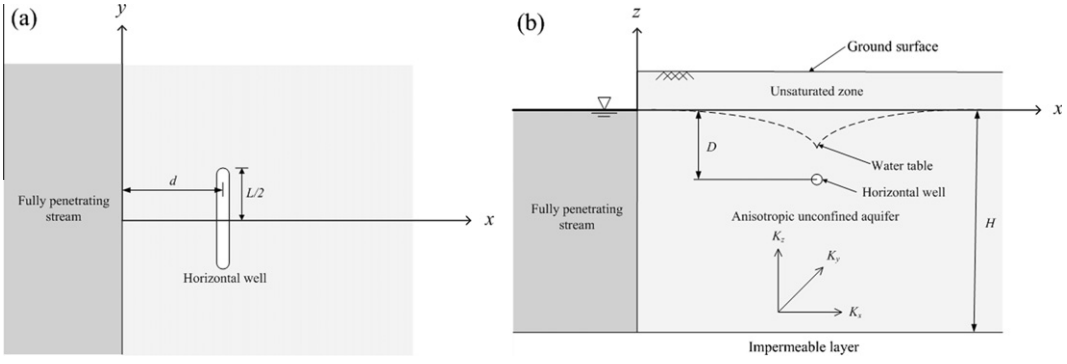

Fig. 1. Schematic diagrams of an unconfined aquifer with a horizontal well near a stream. (a) Top view, (b) cross section view.

Based on the following dimensionless variables [14]:

$$x_D=\frac{x}{H},\quad y_D=\frac{y}{H},\quad z_D=\frac{z}{H},\quad x_{0D}=\frac{x_0}{H},\quad y_{0D}=\frac{y_0}{H},\quad z_{0D}=\frac{z_0}{H},$$
$$d_D=\frac{d}{H},\quad D_D=\frac{D}{H},\quad t_D=\frac{K_x}{H^2S_s}t,\quad h_D=\frac{\pi K_xH}{Q}h, \tag{9}$$

where the subscript D denotes a dimensionless symbol, Eq. (1) can be expressed as

$$\frac{\partial^2 h_D}{\partial x_D^2}+\kappa_y\frac{\partial^2 h_D}{\partial y_D^2}+\kappa_z\frac{\partial^2 h_D}{\partial z_D^2}=\frac{\partial h_D}{\partial t_D}+\pi\delta(x_D-x_{0D})\delta(y_D-y_{0D})\delta(z_D+z_{0D}), \tag{10}$$

where $\kappa_y = K_y/K_x$ and $\kappa_z = K_z/K_x$.

Accordingly, the initial and boundary conditions are denoted as

$$h_D=0 \quad \text{at } t_D=0, \tag{11}$$
$$h_D=0 \quad \text{at } x_D=0, \tag{12}$$
$$\lim_{x_D\to\infty} h_D=0, \tag{13}$$
$$\lim_{y_D\to\pm\infty} h_D=0, \tag{14}$$
$$\frac{\partial h_D}{\partial z_D}=0 \quad \text{at } z_D=-1, \tag{15}$$
$$\alpha\frac{\partial h_D}{\partial t_D}=-\kappa_z\frac{\partial h_D}{\partial z_D} \quad \text{at } z_D=0, \tag{16}$$

where $\alpha = S_y/(S_sH)$.

2.2. Head distribution solutions

Applying Fourier and Laplace transforms to Eqs. (10)–(16) and then inverting the result yield the point source solution shown below. Readers can refer to Appendix A for the detailed derivation.

$$h_a=\frac{4}{\pi}\int_0^\infty\int_0^\infty\left(\Phi_a+\sum_{n=1}^\infty\Psi_a\right)\sin(wx_D)\cos[(y_D-y_{0D})\xi]d\xi dw \quad \text{for } -D_D\leqslant z_D\leqslant 0, \tag{17}$$

$$h_b=\frac{4}{\pi}\int_0^\infty\int_0^\infty\left(\Phi_b+\sum_{n=1}^\infty\Psi_b\right)\sin(wx_D)\cos[(y_D-y_{0D})\xi]d\xi dw \quad \text{for } -1\leqslant z_D\leqslant -D_D, \tag{18}$$

with

$$\Phi_a=\frac{\gamma_0\cosh[\beta_0(1-z_{0D})](e^{-\lambda_0 t_D}-1)}{\lambda_0\eta_0}, \tag{19}$$
$$\Psi_a=\frac{\gamma_n\cos[\beta_n(1-z_{0D})](e^{-\lambda_n t_D}-1)}{\lambda_n\eta_n}, \tag{20}$$
$$\Phi_b=\frac{\gamma_0\cosh[(1+z_D)\beta_0](e^{-\lambda_0 t_D}-1)}{\lambda_0\eta_0}, \tag{21}$$
$$\Psi_b=\frac{\gamma_n\cos[(1+z_D)\beta_n](e^{-\lambda_n t_D}-1)}{\lambda_n\eta_n}, \tag{22}$$
$$\lambda_0=w^2+\kappa_y\xi^2-\kappa_z\beta_0^2, \tag{23}$$
$$\lambda_n=w^2+\kappa_y\xi^2+\kappa_z\beta_n^2, \tag{24}$$
$$\eta_0=\kappa_z\beta_0(1+2\alpha)\cosh\beta_0+[\kappa_z-\alpha\lambda_0]\sinh\beta_0, \tag{25}$$
$$\eta_n=\kappa_z\beta_n(1+2\alpha)\cos\beta_n+[\kappa_z-\alpha\lambda_n]\sin\beta_n, \tag{26}$$
$$\gamma_0=\sin(wx_{0D})[\kappa_z\beta_0\cosh(\beta_0 z_D)+\alpha\lambda_0\sinh(\beta_0 z_D)], \tag{27}$$
$$\gamma_n=\sin(wx_{0D})[\kappa_z\beta_n\cos(\beta_n z_D)+\alpha\lambda_n\sin(\beta_n z_D)], \tag{28}$$

where w and ξ are the dummy variables for Fourier sine and Fourier transform, respectively; the subscripts a and b represent the solution for the aquifer above and below the horizontal well, respectively; β_0 and β_n are respectively the roots of following two equations

$$e^{2\beta_0}=\frac{\kappa_z\beta_0-\alpha\lambda_0}{\kappa_z\beta_0+\alpha\lambda_0}, \tag{29}$$
$$\tan\beta_n=-\frac{\alpha\lambda_n}{\kappa_z\beta_n}. \tag{30}$$

Note that Eq. (30) has infinite roots due to the periodical function $\tan\beta_n$. The roots of these two equations are easily found by Newton's method [15]. Only the positive roots of these two equations are chosen for evaluation. The suggested initial guesses for β_0 and β_n are $[\kappa_z+\sqrt{\kappa_z^2+4\kappa_z\alpha^2(w^2+\kappa_y\xi^2)}]/(2\alpha\kappa_z)$ and $(2n-1)\pi/2$, respectively, where n is an integer from $1, 2, 3, \ldots, \infty$. For the reason of choosing the positive roots, please refer to Appendix C.

The solution of the head distribution for pumping from a horizontal well can then be acquired by integrating the point source solution, Eqs. (17) and (18), along the well axis and then multiplying a reciprocal of well length [e.g., 13,18,19]. The point source therefore becomes a line sink representing a horizontal well along which the uniform pumping rate is Q/L_D. The solution for such a horizontal well is expressed as

$$h_{Da}=\frac{1}{L_D}\int_{-L_D/2}^{L_D/2}h_a dy_{0D} \quad \text{for } -D_D\leqslant z_D\leqslant 0, \tag{31}$$
$$h_{Db}=\frac{1}{L_D}\int_{-L_D/2}^{L_D/2}h_b dy_{0D} \quad \text{for } -1\leqslant z_D\leqslant -D_D. \tag{32}$$

Eq. (31) developed based on Eq. (17) implicitly includes Φ_a and Ψ_a while Eq. (32) developed from Eq. (18) implicitly includes Φ_b and Ψ_b. Note that x_{0D} and z_{0D} in Φ_a, Ψ_a, Φ_b and Ψ_b should be replaced by d_D and D_D, respectively.

2.3. Stream depletion rate

Based on Darcy's law, the infiltration rate from the stream can be written as

$$q=\int_{\Omega_y}\int_{\Omega_z}K_x i dz_D dy_D \quad \text{at } x_D=0, \tag{33}$$

where i represents hydraulic gradient in x direction; Ω_y and Ω_z are the whole domain of the stream in y and z direction, respectively. In the case that the stream fully penetrates the aquifer, substituting $i = \partial h_{Db}/\partial x_D$ for $-1\leqslant z_D\leqslant D_D$ and $i = \partial h_{Da}/\partial x_D$ for $D_D\leqslant z_D\leqslant 0$ into Eq. (33) yields the stream depletion rate as

$$SDR=\frac{q}{Q}=\frac{1}{\pi}\int_{-\infty}^{\infty}\left(\int_{-1}^{-D_D}\frac{\partial h_{Db}}{\partial x_D}dz_D+\int_{-D_D}^{0}\frac{\partial h_{Da}}{\partial x_D}dz_D\right)dy_D \quad \text{at } x_D=0. \tag{34}$$

Eq. (34) implicitly includes D_D in Φ_a, Ψ_a, Φ_b and Ψ_b, indicating that the stream depletion rate in unconfined aquifers is dependent of the depth of the horizontal well.

2.4. A special case: Tsou et al.'s solution [14]

If $S_y = 0$ (i.e., $\alpha = 0$), the present solution, Eqs. (17) and (18), reduces to Tsou et al.'s solution [14] which describes groundwater flow induced from a point source in confined aquifers. For the detailed derivation, readers can refer to Appendix B.

Based on Darcy's law, the stream depletion rate from a horizontal well for Tsou et al.'s solution [14] is expressed as

$$SDR=\frac{2}{\pi^2 L_D}\int_{-L_D/2}^{L_D/2}\int_{-\infty}^{\infty}\int_0^\infty\int_0^\infty\frac{w\sin(wx_{0D})\cos[(y_D-y_{0D})\xi]\left(e^{-(w^2+\kappa_y\xi^2)t_D}-1\right)}{w^2+\kappa_y\xi^2}d\xi dw dy_D dy_{0D}. \tag{35}$$

Note that the stream depletion rate in confined aquifers is independent of the well depth because of no D_D in Eq. (35).

3. Results and discussion

The numerical integrations for Eqs. (31), (32) and (34) can be done by Gaussian quadrature [5, p. 301]. The integrands in these three equations have oscillatory patterns with consecutive roots determined by $\cos[(y_D - y_{0D})\xi] = 0$. Each area between two consecutive roots is evaluated by the 16-term Gaussian quadrature formula. The result of the numerical integration is equal to the total areas which is the sum of each area along the ξ axis. Accordingly, the total areas can be expressed in terms of an infinite series. The series converges quite fast and usually takes only few terms to achieve accuracy to centimeter.

3.1. Effect of specific yield on stream depletion rate

The unconfined aquifer has an effect of instantaneous drainage from water table on the stream depletion rate. Consider that the aquifer has anisotropic hydraulic conductivity falling in the range of 0.01–100 m/day if the aquifer consists of silty sand [4, p.604]. The other parameter values used for evaluation are shown in Table 1. Fig. 2 shows the stream depletion rate obtained from Eq. (34) versus dimensionless time t_D for various S_y (= 0.1 and 0.3). The curves exhibit three segments: rapid increase at early time, middle flat stage, and rapid increase again at late time. The curve with larger S_y has longer flat stage. The first and third segments indicate that the flow from the stream increases with time. However, in the second segment the stream depletion rate maintains constant, indicating that the pumping well obtains the water from the pore

Table 1
The default dimensional value for each parameter.

Parameter	Value
K_x (m/day)	1
K_y (m/day)	1
K_z (m/day)	0.1
S_s (m^{-1})	10^{-5}
S_y	0.3
Q (m^3/day)	100
H (m)	10
D (m)	8
d (m)	40
L (m)	50
t (day)	2

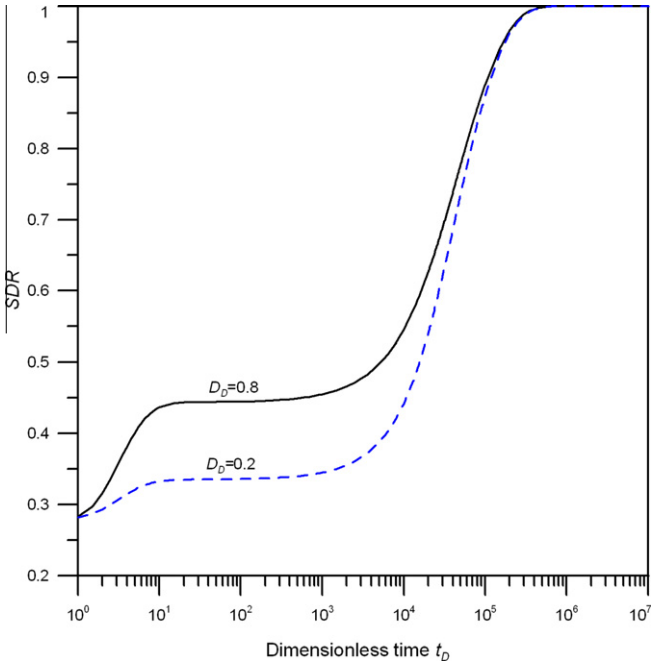

Fig. 3. The temporal stream depletion rate for $D_D = 0.2$ and 0.8.

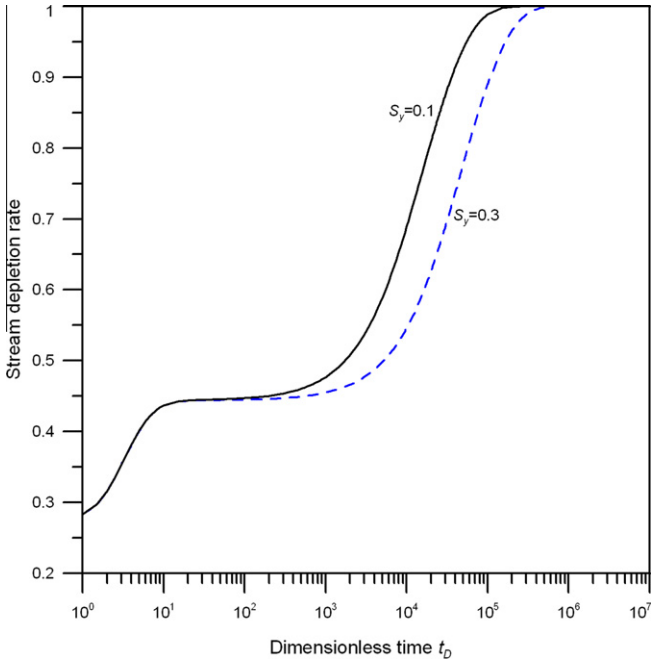

Fig. 2. The temporal stream depletion rate for $S_y = 0.1$ and 0.3.

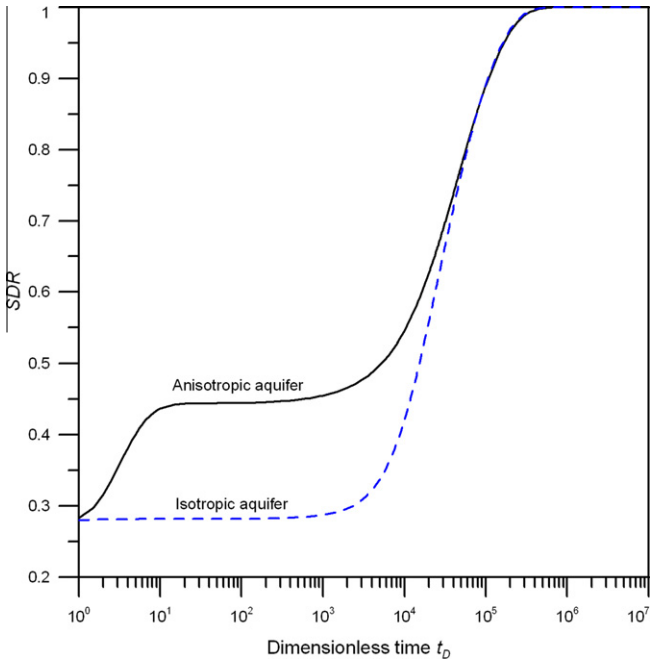

Fig. 4. The temporal stream depletion rate for isotropic and anisotropic aquifers.

drainage. When the dimensionless time is larger than 3×10^5, the stream depletion rate curve of $S_y = 0.1$ approaches one, implying that the water all comes from the stream. In addition, the figure indicates that a larger specific yield ($S_y = 0.3$) leads to a less stream depletion rate after the second segment.

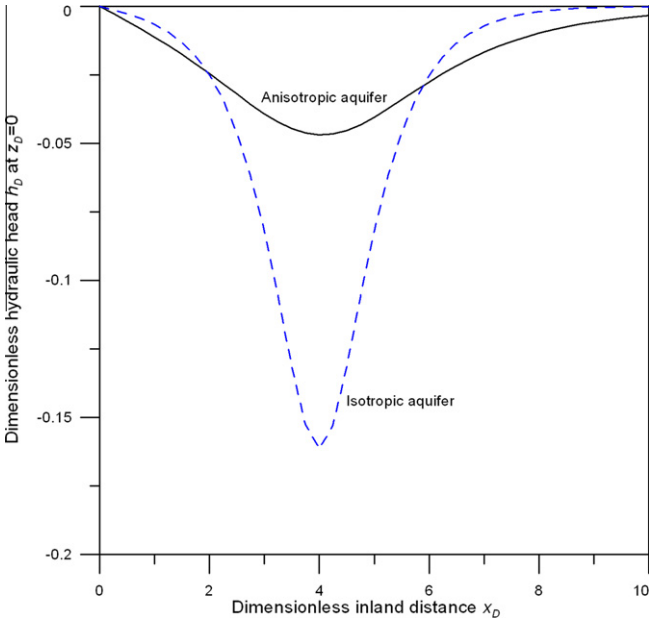

Fig. 5. The spatial water table distribution at $y_D = 0$ for isotropic and anisotropic aquifers.

3.2. Effect of well depth on stream depletion rate and head distribution

The stream depletion rate for unconfined aquifers is dependent of the depth of the horizontal well. Fig. 3 shows stream depletion rate versus dimensionless time t_D for shallow well ($D_D = 0.2$) and deep well ($D_D = 0.8$), indicating that the deep well has a larger stream depletion rate. On the other hand, the shallow well requires longer time to acquire the same amount of stream water as the deep one.

3.3. Effect of anisotropy on stream depletion rate and head distribution

Generally speaking, an anisotropic aquifer has smaller vertical hydraulic conductivity than horizontal one. The value of K_z has an effect on stream depletion rate and head distribution. Consider that an isotropic aquifer has $K_x = K_y = K_z = 1$ m/day and an anisotropic aquifer has $K_x = K_y = 1$ m/day and $K_z = 0.1$ m/day. The comparison of stream depletion rate between these two aquifers shown in Fig. 4 indicates that the anisotropic aquifer has larger stream depletion rate than the isotropic one. This is because smaller K_z makes less water form pore drainage and more water from the stream. A shallow drawdown cone can therefore be expected for the anisotropic aquifer as shown in Fig. 5.

3.4. Spatial head distribution for various depths

Figs. 6 and 7 demonstrate spatial head distribution predicted from Eq. (31) for $z_D = 0$ and $z_D = -D_D$, respectively. For fixed x_D and y_D, the head at $z_D = -D_D$ is smaller than that at $z_D = 0$, indicating that the aquifer has downward flow induced from a pumping

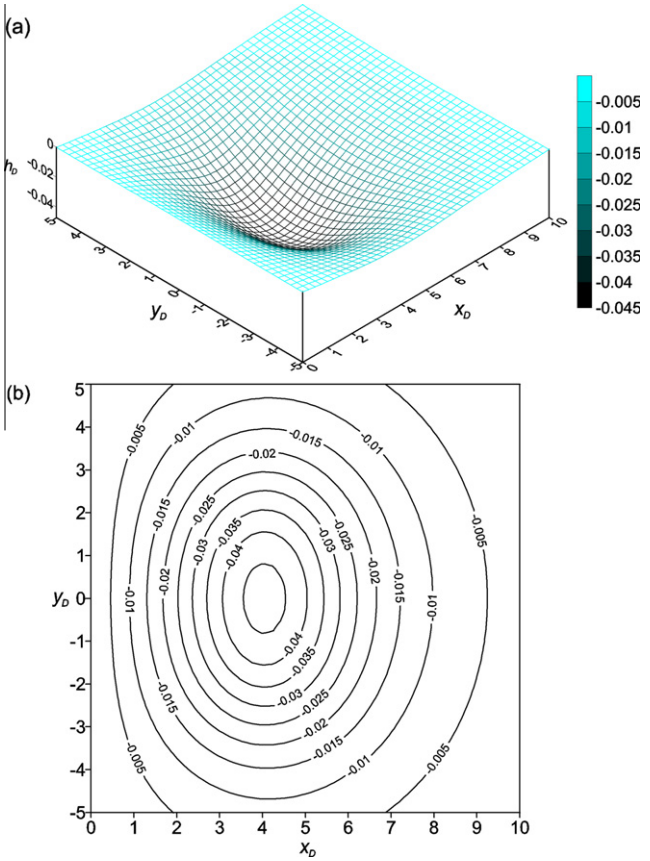

Fig. 6. The spatial water table distribution for (a) 3D view and (b) top view.

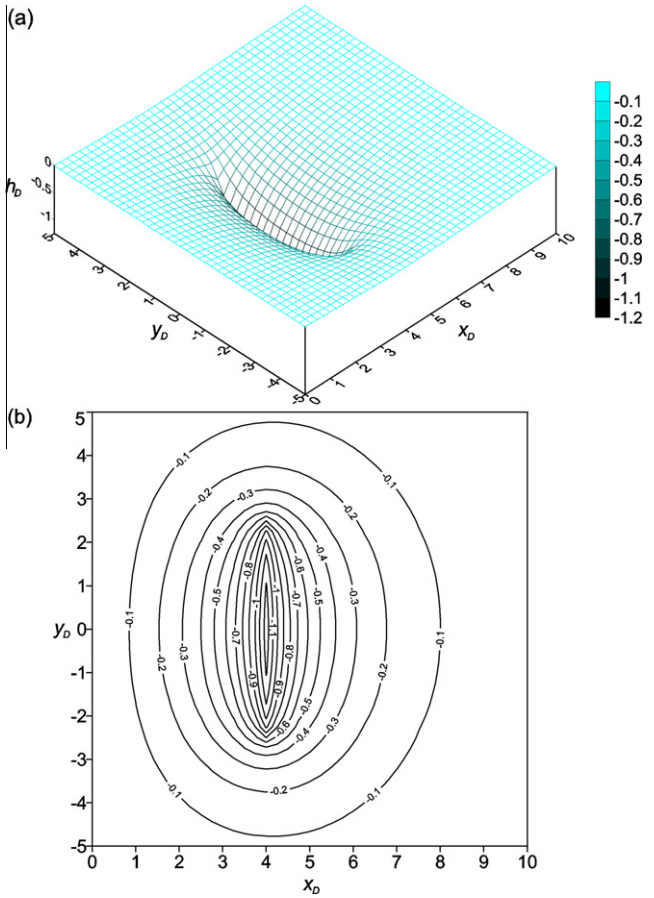

Fig. 7. The spatial head distribution at $z_D = -D_D$ for (a) 3D view and (b) top view.

horizontal well. The minimum head occurs at the center of the horizontal well ($x_D = 4$, $y_D = 0$, $z_D = -D_D$). It is interesting to note that the head distribution shown in Fig. 7 can reflect a line sink (horizontal well) obviously where the head changes dramatically.

3.5. Potential applications of the present solution

The present solutions can be applied to various types of groundwater problems associated with pumping in unconfined aquifers. For example, the present point source solution can also be used to develop the solutions for different type of wells such as slanted well and vertical well with full or partial penetration when integrating Eqs. (17) and (18) along the well axis. In addition, if the stream is located very far away from the well so that the drawdown cone never reaches the stream, the result evaluated from the present solution reduces to that of Zhan and Zlotnik's solution [19, Eq. (23)] describing the head distribution for the aquifer of infinite extent in the horizontal direction. Fig. 8 shows a comparison of spatial head distributions at $y_D = 0$ predicted by the present solution and Zhan and Zlotnik's solution [19]. This figure indicates that the drawdown cone has not reached the stream and the present solution has a good agreement with Zhan and Zlotnik's solution [19].

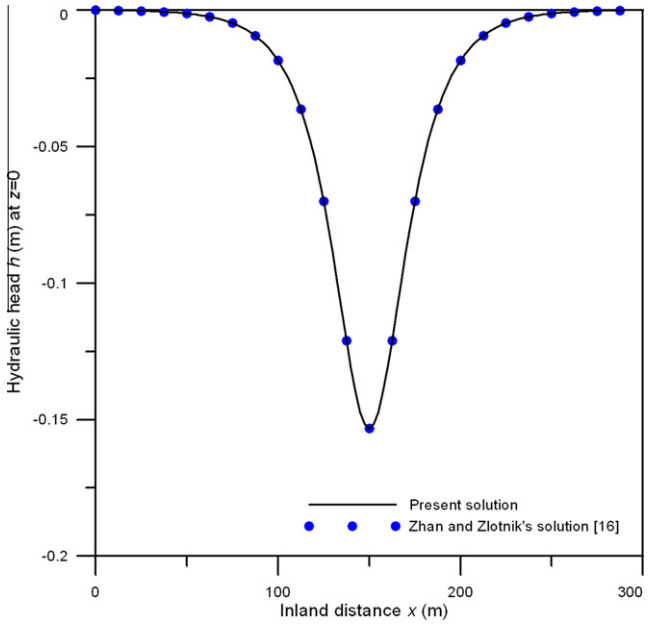

Fig. 8. Comparison between the predicted head by the present solution and Zhan and Zlotnik's solution [19].

Table 2
The field data and aquifer parameters [12].

Parameter	Value
K_x (m/day)	10
K_y (m/day)	10
K_z (m/day)	0.06
S_s (m^{-1})	0.033
S_y	0.3
H (m)	5
D (m)	4.85
d (m)	350
L (m)	300
x (m)	350
z (m)	−4.85

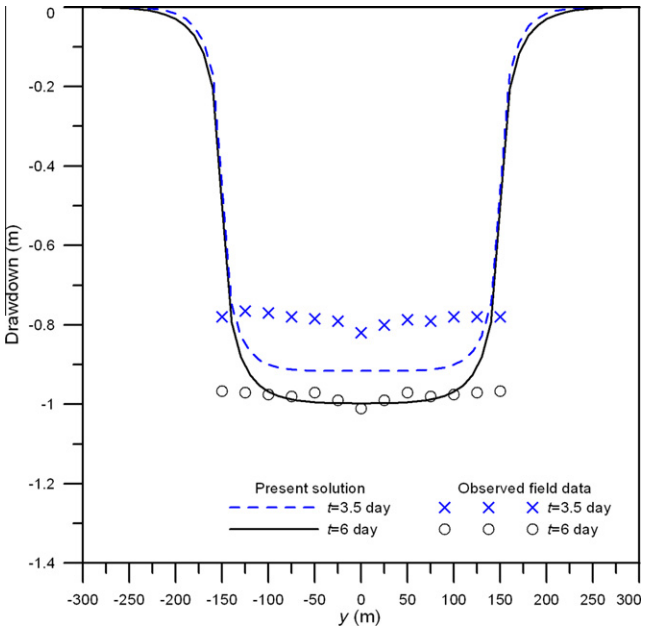

Fig. 9. The predicted drawdown from present solution and observed drawdown from Mohamed and Rushton [12].

3.6. Comparison of present solution with observed field data

Mohamed and Rushton [12] carried out a field experiment with a horizontal well in a shallow aquifer in Sarawak, Malaysia. The aquifer can be considered to extend infinitely in the horizontal direction because the drawdown cone never reaches the boundary of the aquifer during early pumping period. The measured pumping rates are 230 m^3/day at 1.25 day, 160 m^3/day at 3.875 day, and 280 m^3/day at 4.5 day. In fact, the designed pumping rate is 240 m^3/day for long-term water requirement. The other field data and aquifer parameters are listed in Table 2. Fig. 9 shows the observed field data taken from Sarawak [12] and the predicted drawdown from the present solution based on the designed pumping rate and data given in Table 2. The figure shows that the predicted drawdown from present solution has a good agreement with the observed drawdown at $t = 6$ days except at the middle and ends of the well ($y = -150$, 0, 150 m). This discrepancy may mainly arise from the energy loss at the caisson (middle) and the entrance loss at the ends of the field well. However, the predicted drawdown from present solution is obviously smaller than the observed drawdown at $t = 3.5$ days. The differences may come from the fact that the present solution is evaluated based on the designed pumping rate of 240 m^3/day which is larger than the measured early pumping rates given above.

4. Concluding remarks

A general analytical solution is developed for describing flow to a horizontal well. The stream bed is assumed to have the same hydraulic conductivity as the aquifer and the stream is considered to maintain a constant stage during the pumping period. The present solution reduces to Tsou et al.'s solution [14] if the specific yield equals zero. Moreover, the present solution will give good approximation to Zhan and Zlotnik's solution [19] if the pumping well is located far away from the stream. It is found that a larger specific yield of an unconfined aquifer results in a longer middle flat stage and a less stream depletion rate to the pumping horizontal well. An unconfined aquifer with a deeper horizontal well has more stream depletion rate than those with a shallower one. An

aquifer with a smaller vertical hydraulic conductivity produces more stream depletion rate and shallower drawdown cone to the aquifer. In addition, the predicted drawdown from the present solution agrees with the observed drawdown in a horizontal well reported in Mohamed and Rushton [12].

Acknowledgements

This study was supported by the Taiwan National Science Council under the grants NSC 99-NU-E-009-001 and NSC 99-2221-E-009-062-MY3 as well as the "Aim for the Top University Plan" of the National Chiao Tung University and Ministry of Education, Taiwan. The authors would like to thank four anonymous reviewers for their valuable and constructive comments.

Appendix A. The derivation of Eqs. (17) and (18)

Applying Fourier sine, Fourier and Laplace transforms to Eqs. (10)–(16) results in an ordinary differential equation (ODE) and boundary conditions in terms of z_D as

$$\kappa_z \frac{\partial^2 \bar{h}_D}{\partial z_D^2} - (w^2 + \kappa_y \xi^2 + p)\bar{h}_D = \frac{1}{p} e^{i\xi y_{0D}} \sin(w x_{0D}) \delta(z_D + z_{0D}), \quad (A.1)$$

$$\frac{\partial \bar{h}_D}{\partial z_D} = 0 \quad \text{at } z_D = -1, \quad (A.2)$$

$$\kappa_z \frac{\partial \bar{h}_D}{\partial z_D} = -\alpha p \bar{h}_D \quad \text{at } z_D = 0, \quad (A.3)$$

where w, ξ, p are the variables of the Fourier sine, Fourier and Laplace transform, respectively. Due to Dirac delta function, Eq. (A.1) is divided into the two homogeneous ODEs as

$$\kappa_z \frac{\partial^2 \bar{h}_{Da}}{\partial z_D^2} - (w^2 + \kappa_y \xi^2 + p)\bar{h}_{Da} = 0 \quad \text{for } -z_{0D} \leqslant z_D \leqslant 0, \quad (A.4)$$

$$\kappa_z \frac{\partial^2 \bar{h}_{Db}}{\partial z_D^2} - (w^2 + \kappa_y \xi^2 + p)\bar{h}_{Db} = 0 \quad \text{for } -1 \leqslant z_D \leqslant -z_{0D}. \quad (A.5)$$

There are two continuity requirements at $z_D = -z_{0D}$. One is the continuity of the hydraulic head expressed as

$$\bar{h}_{Da} = \bar{h}_{Db} \quad \text{at } z_D = -z_{0D}. \quad (A.6)$$

Integrating Eq. (A.1) from $z_D = -z_{0D}^-$ to $z_D = -z_{0D}^+$ obtains the other continuity requirement which reflects hydraulic gradient discontinuity as

$$\frac{\partial \bar{h}_{Da}}{\partial z_D} - \frac{\partial \bar{h}_{Db}}{\partial z_D} = \frac{1}{p} e^{i\xi y_{0D}} \sin(w x_{0D}) \quad \text{at } z_D = -z_{0D}. \quad (A.7)$$

Solving Eqs. (A.4) and (A.5) with boundary conditions, Eqs. (A.2) and (A.3), as well as continuity requirements, Eqs. (A.6) and (A.7), simultaneously results in

$$\bar{h}_{Da} = G(p) \cdot K_a(p) \quad \text{for } -z_{0D} \leqslant z_D \leqslant 0, \quad (A.8)$$

$$\bar{h}_{Db} = G(p) \cdot K_b(p) \quad \text{for } -1 \leqslant z_D \leqslant -z_{0D}, \quad (A.9)$$

where

$$G(p) = \frac{1}{p}, \quad (A.10)$$

$$\lambda = \sqrt{\frac{w^2 + \kappa_y \xi^2 + p}{\kappa_z}}. \quad (A.13)$$

Taking inverse Laplace transform to Eq. (A.10) yields

$$g(t_D) = L^{-1}\{G(p)\} = 1, \quad (A.14)$$

where $L^{-1}\{\}$ represents inverse Laplace transform.

Both Eqs. (A.11) and (A.12) are a single value function. Based on Bromwich integral, the results of inverse Laplace transform for these two equations can therefore be, respectively, expressed as

$$k_a(t_D) = \frac{1}{2\pi i} \int_{r-i\infty}^{r+i\infty} K_a(p) e^{p t_D} dp, \quad (A.15)$$

$$k_b(t_D) = \frac{1}{2\pi i} \int_{r-i\infty}^{r+i\infty} K_b(p) e^{p t_D} dp, \quad (A.16)$$

where i is an imaginary unit and r is a real constant which is so large that all of the real parts of the singularities are smaller than it. The pathway of Bromwich integral contains a close contour with a semicircle and straight line parallel to the imaginary axis. According to Jordan's Lemma, the value of the integration for the semicircle tends to zero if its radius approaches infinity. Based on the residue theory, the result of the integration for Eqs. (A.15) and (A.16) can be expressed as summation of the residue for each pole. Therefore, $k_a(t_D)$ and $k_b(t_D)$ can respectively be further expressed as

$$k_a(t_D) = \sum_{N=1}^{\infty} \text{Res}\Big|_{p=p_N}, \quad (A.17)$$

$$k_b(t_D) = \sum_{N=1}^{\infty} \text{Res}\Big|_{p=p_N}, \quad (A.18)$$

where p_N is the pole in complex plane and *Res* represents the residue for each pole.

Let the denominator of Eq. (A.11) or (A.12) equal zero and the roots of this equation represent the location of poles in complex plane. Note that the poles exist only at the real axis. Only one pole, p_0, exists between $p = 0$ and $p = -w^2 - \kappa_y \xi^2$ while infinite poles, p_n, happen behind $p = -w^2 - \kappa_y \xi^2$.

For the residue without imaginary unit, the pole at $p = p_0$ should be expressed as $p_0 = \kappa_z \beta_0 - \kappa_y \xi^2 - w^2$ obtained from letting $\lambda = \beta_0$. Similarly, the poles at $p = p_n$ is expressed as $p_n = -\kappa_z \beta_n - \kappa_y \xi^2 - w^2$ obtained from letting $\lambda = i\beta_n$. Substituting $\lambda = \beta_0$ and $p = p_0 = \kappa_z \beta_0 - \kappa_y \xi^2 - w^2$ into the denominator of Eq. (A.11) or (A.12) results in Eq. (29). Similarly, substituting $\lambda = i\beta_n$ and $p = p_n = -\kappa_z \beta_n - \kappa_y \xi^2 - w^2$ into denominator of Eq. (A.11) or (A.12) yields Eq. (30).

The residues of Eqs. (A.17) and (A.18) can respectively be determined from the following formulas

$$\text{Res}|_{p=p_N} = \lim_{p \to p_N} K_a(p)\ e^{p t_D}(p - p_N), \quad (A.19)$$

$$\text{Res}|_{p=p_N} = \lim_{p \to p_N} K_b(p)\ e^{p t_D}(p - p_N), \quad (A.20)$$

$$K_a(p) = \frac{\sin(w x_{0D}) \cosh[\lambda(1 - z_{0D})] \text{sech}[\lambda(z_D + z_{0D})][-\kappa_z \lambda \cosh(\lambda z_D) + p\alpha \sinh(\lambda z_D)] e^{i\xi y_{0D}}}{\kappa_z \lambda (p\alpha \cosh\lambda + \kappa_z \lambda \sinh\lambda)}, \quad (A.11)$$

$$K_b(p) = \frac{\sin(w x_{0D}) \cosh[\lambda(1 - z_D)] \text{sech}[\lambda(z_D + z_{0D})][-\kappa_z \lambda \cosh(\lambda z_{0D}) - p\alpha \sinh(\lambda z_{0D})] e^{i\xi y_{0D}}}{\kappa_z \lambda (p\alpha \cosh\lambda + \kappa_z \lambda \sinh\lambda)}, \quad (A.12)$$

Substituting Eqs. (A.11) into Eq. (A.19) and applying L'Hopital's rule results in

$$\mathrm{Res}|_{p=p_N} = \lim_{p\to p_N} \frac{\sin(wx_{0D})\cosh[\lambda(1-z_{0D})][-\kappa_z\lambda\cosh(\lambda z_D)+p\alpha\sinh(\lambda z_D)]e^{i\xi y_{0D}+pt_D}}{\kappa_z\lambda\left(\frac{1}{2}\cosh\lambda+\alpha\cosh\lambda+\frac{\sinh\lambda}{2\lambda}+\frac{p\alpha\sinh\lambda}{2\kappa_z\lambda}\right)}. \tag{A.21}$$

Similarly, substituting Eq. (A.12) into Eq. (A.20) and applying L'Hopital's rule yields

$$\mathrm{Res}|_{p=p_N} = \lim_{p\to p_N} \frac{\sin(wx_{0D})\cosh[\lambda(1-z_D)][-\kappa_z\lambda\cosh(\lambda z_{0D})-p\alpha\sinh(\lambda z_{0D})]e^{i\xi y_{0D}+pt_D}}{\kappa_z\lambda\left(\frac{1}{2}\cosh\lambda+\alpha\cosh\lambda+\frac{\sinh\lambda}{2\lambda}+\frac{p\alpha\sinh\lambda}{2\kappa_z\lambda}\right)}. \tag{A.22}$$

With $p_N = p_0$ and $\lambda = \beta_0$, Eq. (A.21) leads to

$$\mathrm{Res}|_{p=p_0} = -\frac{2\gamma_0\cosh[\beta_0(1-z_{0D})]}{\eta_0}e^{i\xi y_{0D}-\lambda_0 t_D}. \tag{A.23}$$

Similarly, substituting $p_N = p_n$ and $\lambda = i\beta_n$ into Eq. (A.21) results in

$$\mathrm{Res}|_{p=p_n} = -\frac{2\gamma_n\cos[\beta_n(1-z_{0D})]}{\eta_n}e^{i\xi y_{0D}-\lambda_n t_D}. \tag{A.24}$$

Note that the sum of Eqs. (A.23) and (A.24) is the result of integration of Eq. (A.15).

With $p_N = p_0$ and $\lambda = \beta_0$, Eq. (A.22) yields

$$\mathrm{Res}|_{p=p_0} = -\frac{2\gamma_0\cosh[\beta_0(1-z_D)]}{\eta_0}e^{i\xi y_{0D}-\lambda_0 t_D}. \tag{A.25}$$

Similarly, substituting $p_N = p_n$ and $\lambda = i\beta_n$ into Eq. (A.22) yields

$$\mathrm{Res}|_{p=p_n} = -\frac{2\gamma_n\cos[\beta_n(1-z_D)]}{\eta_n}e^{i\xi y_{0D}-\lambda_n t_D}. \tag{A.26}$$

The sum of Eqs. (A.25) and (A.26) is the result of integration of Eq. (A.16).

The results of inverse Laplace transform for Eqs. (A.8) and (A.9) can be obtained, respectively, by the convolution theorem.

$$h_{Da} = \int_0^{t_D} g(t_D-\tau)\cdot k_a(\tau)d\tau, \tag{A.27}$$

$$h_{Db} = \int_0^{t_D} g(t_D-\tau)\cdot k_b(\tau)d\tau. \tag{A.28}$$

The result of integration of Eq. (A.27) leads to the sum of Eqs. (19) and (20) and the result of integration of Eq. (A.28) leads to the sum of Eqs. (21) and (22). The final solutions expressed as Eqs. (17) and (18) can then be obtained after taking inverse Fourier and Fourier sine transform.

Appendix B. The derivation of reducing to Tsou et al.'s solution [14]

Substituting $\alpha = 0$ into Eqs. (29) and (30) yields $e^{2\beta_0} = 1$ and $\tan\beta_n = 0$, respectively. Obviously, the roots of these two equations are $\beta_0 = 0$ and $\beta_n = n\pi$ where n is an integer from $1, 2, 3, \ldots, \infty$. Multiplying the numerator and denominator of Eq. (19) by $1/\beta_0$ and substituting $\alpha = 0$ into Eq. (19) leads to

$$\Phi_a = \frac{\sin(wx_{0D})\cosh(\beta_0 z_D)\cosh[\beta_0(1-z_{0D})]\left(e^{-(w^2+\kappa_y\xi^2-\kappa_z\beta_0^2)t_D}-1\right)}{(w^2+\kappa_y\xi^2-\kappa_z\beta_0^2)\left\{\cosh\beta_0+\frac{\sinh\beta_0}{\beta_0}\right\}}. \tag{B.1}$$

Applying L'Hopital's rule to $\sinh(\beta_0)/\beta_0$ in the denominator of Eq. (B.1) first and then substituting $\beta_0 = 0$ into Eq. (B.1) results in

$$\Phi_a = \frac{\sin(wx_{0D})\left(e^{-(w^2+\kappa_y\xi^2)t_D}-1\right)}{2(w^2+\kappa_y\xi^2)}. \tag{B.2}$$

Alternatively, Eq. (B.2) can be obtained from substituting $\alpha = 0$ and $\beta_0 = 0$ into Eq. (21).

With $\alpha = 0$ and $\beta_n = n\pi$, Eq. (20) leads to

$$\Psi_a = \frac{\sin(wx_{0D})n\pi\cos(n\pi z_D)\cos[n\pi(1-z_{0D})]\left(e^{-(w^2+\kappa_y\xi^2+\kappa_z n^2\pi^2)t_D}-1\right)}{(w^2+\kappa_y\xi^2+\kappa_z\beta_n^2)[n\pi\cos(n\pi)+\sin(n\pi)]}. \tag{B.3}$$

Substituting $\sin(n\pi) = 0$ and $\cos[n\pi(1-z_{0D})] = \cos(n\pi)\cos(n\pi z_{0D}) - \sin(n\pi)\sin(n\pi z_{0D})$ into Eq. (B.3) yields

$$\Psi_a = \frac{\sin(wx_{0D})\cos(n\pi z_D)\cos(n\pi z_{0D})\left(e^{-(w^2+\kappa_y\xi^2+\kappa_z n^2\pi^2)t_D}-1\right)}{w^2+\kappa_y\xi^2+\kappa_z n^2\pi^2}. \tag{B.4}$$

Alternatively, Eq. (B.4) can be obtained after substituting $\alpha = 0$ and $\beta_n = n\pi$ into Eq. (22). Accordingly, Tsou et al.'s solution [14, Eq. (16)] with a point source can be obtained from substituting Eqs. (B.2) and (B.4) into Eq. (17) as

$$\begin{aligned} h_{Tsou}(x_D, y_D, z_D, t_D) &= \frac{2}{\pi}\int_0^\infty\int_0^\infty \sin(wx_D)\cos[(y_D-y_{0D})\xi] \\ &\times\left[\frac{\sin(wx_{0D})\left(e^{-(w^2+\kappa_y\xi^2)t_D}-1\right)}{w^2+\kappa_y\xi^2}\right. \\ &\left.+\sum_{n=1}^{\infty}\frac{2\sin(wx_{0D})\cos(n\pi z_D)\cos(n\pi z_{0D})\left(e^{-(w^2+\kappa_y\xi^2+\kappa_z n^2\pi^2)t_D}-1\right)}{w^2+\kappa_y\xi^2+\kappa_z n^2\pi^2}\right]d\xi\,dw. \end{aligned} \tag{B.5}$$

Appendix C. The reason of choosing positive roots β_0 and β_n

Eqs. (29) and (30) for the roots of β_0 and β_n are derived, respectively, based on setting $\sqrt{(w^2+\kappa_y\xi^2+p)/\kappa_z} = \beta_0$ and $\sqrt{(w^2+\kappa_y\xi^2+p)/\kappa_z} = i\beta_n$. The values of κ_y, κ_z, w and ξ are positive while p is negative. The value of $w^2+\kappa_y\xi^2+p$ could therefore be greater or smaller than zero. We let $\sqrt{(w^2+\kappa_y\xi^2+p)/\kappa_z} = \beta_0$

if $w^2 + \kappa_y\xi^2 + p > 0$ and $\sqrt{(w^2 + \kappa_y\xi^2 + p)/\kappa_z} = i\beta_n$ if $w^2 + \kappa_y\xi^2 + p < 0$. Thus, both β_0 and β_n must be positive for any value of $w^2 + \kappa_y\xi^2 + p$.

References

[1] Butler JJ, Zhan X, Zlotnik VA. Pumping-induced drawdown and stream depletion in a leaky aquifer system. Ground Water 2007;45:178–86. doi:10.1111/j.1745-6584.2006.00272.x.

[2] Chen X, Yin Y. Semi-analytical solutions for stream depletion in partially penetrating streams. Ground Water 2004;42:92–6.

[3] Fox GA, DuChateau P, Durnford DS. Analytical model for aquifer response incorporating distributed stream leakage. Ground Water 2002;40:378–84.

[4] Freeze RA, Cherry JA. Groundwater. New Jersey: Prentice-Hall; 1979.

[5] Gerald CF, Wheatley PO. Applied numerical analysis. 7th ed. California: Addison-Wesley; 2004.

[6] Hunt B. Stream depletion in a two-layer leaky aquifer system. J Hydrol Eng 2009;14:895–903. doi:10.1061/(ASCE)HE.1943-5584.0000063.

[7] Intaraprasong T, Zhan H. A general framework of stream-aquifer interaction caused by variable stream stages. J Hydrol 2009;373:112–21. doi:10.1016/j.jhydrol.2009.04.016.

[8] Joshi SD. Cost/benefits of horizontal wells. Soc Petrol Eng 2003:19–24.

[9] Kawecki MW. Transient flow to a horizontal water well. Ground Water 2000;38(6):842–50.

[10] Kompani-Zare M, Zhan H, Samani N. Analytical study of capture zone of a horizontal well in a confined aquifer. J Hydrol 2005;307:48–59. doi:10.1016/j.hydrol.2004.09.021.

[11] Langseth DE, Smyth AH, May J. A method for evaluating horizontal well pumping tests. Ground Water 2004;42(5):689–99.

[12] Mohamed A, Rushton K. Horizontal wells in shallow aquifers: field experiment and numerical model. J Hydrol 2006;329:98–109. doi:10.1016/j.jhydrol.2006.02.006.

[13] Sun D, Zhan H. Flow to a horizontal well in an aquitard-aquifer system. J Hydrol 2006;321:364–76. doi:10.1016/j.jhydrol.2005.08.008.

[14] Tsou P-R, Feng Z-Y, Yeh H-D, Huang C-S. Stream depletion rate with horizontal or slanted wells in confined aquifers near a stream. Hydrol Earth Syst Sci 2010;14:1477–85. doi:10.5194/hessd-7-2347-2010.

[15] Yeh H-D. Theis' solution by nonlinear least-squares and finite- difference Newton's method. Ground Water 1987;25:710–5.

[16] Yeh H-D, Huang C-S, Chang Y-C, Jeng D-S. An analytical solution for tidal fluctuations in unconfined aquifers with a vertical beach. Water Resour Res 2010;46:W10535. doi:10.1029/2009WR008746.

[17] Yeh H-D, Chang Y-C, Zlotnik VA. Stream depletion rate and volume of flow in wedge-shape aquifers. J Hydrol 2008;349:501–11. doi:10.1016/j.jhydrol.2007.11.025.

[18] Zhan H, Wang LV, Park E. On the horizontal-well pumping tests in anisotropic confined aquifers. J Hydrol 2001;252:37–50.

[19] Zhan H, Zlotnik VA. Ground water flow to horizontal and slanted wells in unconfined aquifers. Water Resour Res 2002;38:1108. doi:10.1029/2001WR000401.

[20] Zhan H, Park E. Hydraulics of horizontal wells in leaky aquifers. J Hydrol 2003;281:129–46.

[21] Zlotnik VA, Tartakovsky DM. Stream depletion by groundwater pumping in leaky aquifers. J Hydrol Eng 2008;13(2):43–50. doi:10.1061/(ASCE)1084-0699(2008)13:2(43).